Available online at www.sciencedirect.com
ScienceDirect
Carbohydrate Research 343 (2008) 1435–1445
Carbohydrate RESEARCH

# Depiction of the forces participating in the 2-*O*-sulfo-α-L-iduronic acid conformational preference in heparin sequences in aqueous solutions

Laercio Pol-Fachin[a] and Hugo Verli[a,b,*]

[a]*Centro de Biotecnologia, Universidade Federal do Rio Grande do Sul, Av Bento Gonçalves 9500, CP 15005, Porto Alegre 91500-970, RS, Brazil*
[b]*Faculdade de Farmácia, Universidade Federal do Rio Grande do Sul, Av Ipiranga 2752, Porto Alegre 90610-000, RS, Brazil*

Received 31 August 2007; received in revised form 3 April 2008; accepted 13 April 2008
Available online 22 April 2008

**Abstract**—2-*O*-Sulfo-α-L-iduronic acid (IdoA2S) is one of the main components of heparin, an anticoagulant and antithrombotic polysaccharide able to potentiate the inhibitory effect of antithrombin over plasma serine proteases. This monosaccharide unit adopts an equilibrium between chair ($^1C_4$) and skew-boat ($^2S_O$) forms as a function of heparin sequence size and composition. Although the prevalence of the $^1C_4$ chair conformation in monosaccharides is understood, the reasons for the increase in $^2S_O$ contribution in the whole polysaccharide chain are still uncertain. In this context, 0.2 μs molecular dynamics simulations of IdoA2S-containing oligosaccharides indicated that stabilization due to intramolecular hydrogen bonds around IdoA2S is highly correlated ($p \leqslant 0.001$) with the expected conformational equilibrium for this residue in solution. This behavior explains the known effect of different heparin compositions, at the monosaccharide level, on IdoA2S conformation in biological solutions.


*Keywords:* Heparin; Molecular dynamics; Polysaccharide; IdoA; Iduronic acid

## 1. Introduction

Heparin, the first compound used clinically as an anticoagulant and antithrombotic agent,[1] is a sulfated polysaccharide composed of (1→4)-linked disaccharide units, mainly containing residues of uronic acids, 2-*O*-sulfo-α-L-iduronic acid (IdoA2S) or non-sulfated β-D-glucuronic acid, and 2,6-di-*O*-sulfo-glucosamine (GlcNS,6S).[2] Through the formation of a ternary complex with antithrombin (AT) and proteases from the blood clotting cascade, heparin potentiates the AT inhibitory effect on these proteases,[3] in a process that appears to be influenced by the unusual flexibility of IdoA2S residues. This monosaccharide unit is capable of adopting an equilibrium between the chair ($^1C_4$) and skew-boat ($^2S_O$) forms,[4] not causing the whole polysaccharide chain to bend and so contributing to unique binding properties.[5]

Although the knowledge of the IdoA2S conformational equilibrium has been known for more than 20 years,[6] an understanding of its driving forces is mostly unknown. Early force field calculations on heparin oligosaccharides pointed out that the 3-*O*-sulfo group on GlcNS residues is capable of promoting small stabilization (0.5 kcal mol$^{-1}$) of the skew-boat conformation on the subsequent IdoA2S residue.[4] However, the assessment of more refined computations capable of providing a comprehensive understanding of IdoA2S conformational equilibrium was, until recently, absent.

The major contribution in this direction was supplied by Hricovíni, using B3LYP/6-311++G** on methyl 2-*O*-sulfo-α-L-iduronate monosodium salt, in a study that was able to reproduce the relative stability expected to

* Corresponding author. Tel.: +55 51 3308 7770; fax: +55 51 3308 7309; e-mail: hverli@cbiot.ufrgs.br

0008-6215/$ - see front matter © 2008 Elsevier Ltd. All rights reserved.
doi:10.1016/j.carres.2008.04.016

occur for this residue in aqueous solution,[7] that is, a great prevalence of the $^{1}C_{4}$ chair conformation in the monosaccharide. These preferences were not reproduced by other authors, who identified the $^{2}S_{O}$ conformation as the preferred form of IdoA2S in solution using the same basis set.[8] Although these results may be explained by the limited set of starting conformations that can be simulated by quantum-mechanical calculations, it points to the potential advantages in employing molecular dynamics (MD) simulations to access a biologically relevant ensemble of conformations, correlated with biological phenomena.

In previous work, our group applied MD simulations to estimate the enthalpic penalty in the interaction of heparin with AT due to conformational modifications of IdoA2S.[9] The results suggested an absence of major conformational requirements, at least at the enthalpic level, on IdoA2S interaction with AT, as both skew-boat and chair conformations contribute with similar enthalpies upon interaction with the target protein. Additionally, these studies suggest that AT may select the predominant IdoA2S solution conformation, as seen in crystallographic data.[10] In a synthetic pentasaccharide, this residue lies almost completely in the skew-boat form when in solution.[11] A similar dynamic recognition was already observed to occur between heparin and FGF-1.[12,13] Nevertheless, the conformational equilibrium of IdoA2S is indeed capable of inducing conformational changes in heparin sequences in solution.[14,15] However, there is still no connection between the recent studies at the monosaccharide level of this residue,[7] where chair forms predominate,[4] and the entire polysaccharide chain, where the skew-boat may contribute from ~40% to 60% of the total IdoA2S conformational preference, depending on the heparin sequence.[4]

In this context, the current work intends to identify the interactions responsible for the IdoA2S conformational equilibrium in heparin sequences. Two models for evaluation of IdoA2S forms were employed: compound **1**, which represents the usual heparin sequences with considerable contributions of the $^{2}S_{O}$ conformation and compound **2**, which represents a heparin sequence with a major contribution of the $^{1}C_{4}$ conformation (Fig. 1). The methodology used includes the calculation of energy contour plots, that is, relaxed maps, associated with heparin oligosaccharides, including IdoA2S in its different solution conformations. The resulting minimum-energy geometries were further refined using a series of 0.2 μs MD simulations in explicit solvent. The results obtained expand information about IdoA2S flexibility from the monosaccharide to the polysaccharide level, contributing to an understanding of the forces responsible for the conformational preferences of this residue in oligosaccharide sequences.

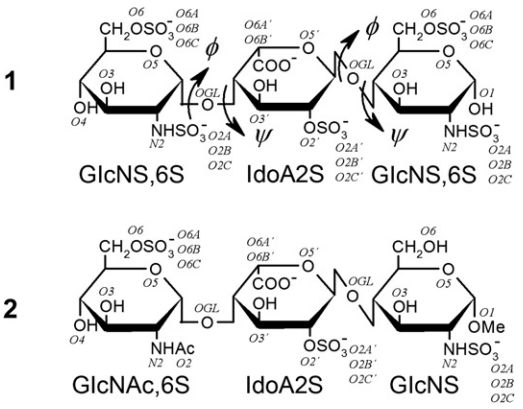


**Figure 1.** The two trisaccharide fragments of heparin, **1** and **2**, constructed based on the dodecasaccharide structure previously determined by NMR.[14]

## 2. Experimental

### 2.1. Computational methods

**2.1.1. Nomenclature and software.** The recommendations and symbols of nomenclature as proposed by IUPAC[16] are used. The relative orientation of a pair of contiguous carbohydrate residues is described by two torsional angles at the glycosidic linkage, denoted $\phi$ and $\psi$. For a (1→4) linkage, the definitions are those shown in Eqs. 1 and 2:

$$\phi = \text{O-5–C-1–O-1–C-4}' \quad (1)$$

$$\psi = \text{C-1–O-1–C-4}'\text{–C-5}' \quad (2)$$

All disaccharide topologies were generated with the PRODRG server,[17] manipulation of structures was performed with MOLDEN[18] and all the MD calculations and analysis were performed using GROMACS simulation suite [19] employing GROMOS96 force field as previously described.[9,15,20]

**2.1.2. Topology construction.** The heparin fragment under the 1HPN PDB code[14] was retrieved to be used on this work. The dodecassaccharide was reduced to the disaccharide units included in compounds **1** (GlcNS,6S–IdoA2S and IdoA2S–GlcNS,6S) and **2** (GlcNAc,6S–IdoA2S and IdoA2S–GlcNS), as illustrated in Figure 1. Although **1** shows a conformational distribution of its IdoA2S residue between $^{1}C_{4}$ and $^{2}S_{O}$ states in amounts of 60% and 40%, respectively,[4] compound **2** presents only the $^{1}C_{4}$ conformation in aqueous solutions.[21] These structures were then submitted to the PRODRG server and the initial geometries and crude topologies were retrieved. These two PRODRG topology files were used to describe properly the different conformational state of IdoA2S ($^{1}C_{4}$ or $^{2}S_{O}$) and GlcNS residues ($^{4}C_{1}$) through improper dihedrals.[15] Based on such an approach, it is possible to control the conforma-

tion adopted in solution by the monosaccharide residue and so identify the effect of these conformations on the properties under investigation. As a consequence, any conformational transition observed during MD trajectories is due to the exocyclic dihedral of the represented hexopyranoses. The HF/6-31G** derived Löwdin atomic charges were employed,[15,20] while the reference bond lengths were adjusted to those observed in NMR data under the 1HPN PDB code.[14]

**2.1.3. Calculation of energy contours.** The conformational description for compounds **1** (GlcNS,6S–IdoA2S and IdoA2S–GlcNS,6S) and **2** (GlcNAc,6S–IdoA2S and IdoA2S–GlcNS) glycosidic linkages was performed by varying the $\phi$ and $\psi$ angles from $-180$ to 180 degrees with a 30 degree step, in a total of 144 conformers for each linkage. This was performed by using a 334.8 kJ mol$^{-1}$ constant force to restrict only the $\phi$ and $\psi$ proper dihedrals during energy minimization in each of the above-mentioned values, allowing the search of the conformational space associated with the disaccharide. Then, using the minimized output conformation, a series of MD simulations were performed for 35 ps at 10 K, with an integration step of 0.5 fs to further support the search for minimum-energy conformations. In this process, the rotatable exocyclic groups were allowed to freely search for minimum-energy orientations. The relative stabilities of each conformation, obtained from the 10 K MD last frame, based on GROMOS96 force field and HF/6-31G** Löwdin atomic charges, were used to construct relaxed energy contour plots describing the conformation of each glycosidic linkage of **1** and **2** as a function of IdoA2S conformation.

**2.1.4. MD simulations.** The minimum-energy conformations obtained from the energy maps were submitted to a 0.2 μs MD simulation in aqueous solution using the SPC water model. A triclinic water box under periodic boundary conditions was employed, using a 10 Å minimum distance from solute to the box faces. Counter ions ($Na^+$) were added to neutralize the system charge. The employed MD protocol was based on previous studies,[22] as described.[9,15,20] The Lincs method[23] was applied to constrain covalent bond lengths, allowing an integration step of 2 fs after an initial energy minimization using the Steepest Descents algorithm. All simulations applied the Particle-Mesh Ewald method,[24] while Coulomb and van der Waals cut-offs were adjusted to 9 Å.

Temperature and pressure were kept constant by coupling carbohydrate, ions, and solvent to external temperature and pressure baths with coupling constants of $\tau = 0.1$ and 0.5 ps, respectively. The dielectric constant was treated as $\varepsilon = 1$, and the reference temperature was adjusted to 310 K. The systems were heated slowly from 50 to 310 K, in steps of 5 ps, each one increasing the reference temperature by 50 K. A reference value of 3.5 Å between heavy atoms was considered for hydrogen bonds,[25] and a cutoff angle of 60° between hydrogen-donor–acceptor.[19] The structure of the solvent around heparin disaccharides was analyzed through calculation of radial distribution functions and residence times of water molecules around solute polar atoms.[19]

Average inter-residue interaction energies were obtained from the 0.2 μs MD simulations in the presence of explicit solvent molecules ($N = 200{,}001$). Data were evaluated by Kruskal–Wallis One-Way Analysis of Variance (ANOVA) on Ranks, and all pair-wise multiple comparisons were evaluated by the Tukey Test. Additionally, comparisons between two groups were evaluated by the Mann–Whitney Rank Sum Test. All statistical calculations were performed using SIGMASTAT for Windows, version 3.5.

## 3. Results and discussion

### 3.1. Dynamics of linkages between IdoA2S and GlcNS,6S

Although the IdoA2S conformational equilibrium has already been determined in solution,[4] its influence upon complexation to target proteins is uncertain. While several proteins had been already structurally characterized in complex with oligosaccharide sequences containing IdoA2S, these target receptors appear to show no common specific geometric requirement, as both $^1C_4$ (as shown in 1AXM,[26] 1FQ9,[27] 2BRS,[28] 1G5N,[29] 1GMN,[30] and 1E0O[31] crystallographic complexes with different target receptor, 2ERM,[32] a FGF-1 complex with heparin determined by NMR methods, and 1HPN,[14] a single NMR conformation of an unbounded heparin dodecasaccharide) and $^2S_O$ (as shown in 1G5N,[29] 1GMN,[30] 1E0O,[31] 1RID,[33] and 1E03[10] crystallographic complexes with different target receptor, 2ERM,[32] a FGF-1 complex with heparin determined by NMR methods, and 1HPN,[14] a NMR conformation of an unbounded heparin dodecasaccharide) forms of this residue are observed in the three-dimensional structures, as compared elsewhere.[34] Indeed, there are complexes in which both chair and skew-boat IdoA2S conformations are observed, as it is the case for annexin V,[29] NK1,[30] and fibroblast growth factor.[31,32] Based on these data, it becomes clear that both $^1C_4$ and $^2S_O$ conformations of IdoA are capable of being retained in three-dimensional structures, both from crystallographic and solution sources, which may depend on either receptor specificity or predominance in solution.

Regarding the expected influence of IdoA2S over heparin conformation,[5] a recent analysis[34] compared the experimental information about its conformations when bound to different proteins, including both NMR and X-ray-derived complexes. These data may provide a

quantitative estimation of IdoA2S conformational influence over polysaccharide flexibility by describing the amplitude of the conformations adopted by heparin when complexed to its different target receptors. Accordingly, this analysis[34] reported that GlcNS,6S–IdoA2S dihedral flexibility is increased upon transition from a $^1C_4$ chair to a $^2S_O$ skew-boat at the $\psi$ angle (Table 1). However, the molecular origins of this flexibility are not clear, nor are the reasons for the displacement of a conformational equilibrium mainly centered in the $^1C_4$ chair to a progressive contribution of a $^2S_O$ conformation as a consequence of sequence size and composition. A complete understanding of the conformational and structural features of heparin will certainly support the design of new antithrombotic agents capable of reproducing the pharmacological activity of this polysaccharide through mimicking its bioactive conformation. Therefore, to look for the forces that contribute in IdoA2S conformational equilibrium between $^1C_4$ and $^2S_O$ conformations, as well as its influence on global heparin conformation, we calculated relaxed contour plots for disaccharides representing the minimum heparin-composing units (Fig. 2).

The first aspect to be noted on the plots presented in Figure 2 is related to the flexibility around the heparin glycosidic linkages. In agreement with the data obtained from experimental data comparisons,[34] the GlcNS,6S-(1→4)-IdoA2S linkage with IdoA2S in the $^2S_O$ conformation presents a large minimum-energy region compared to the linkage presenting the $^1C_4$ conformation and, consequently, greater flexibility and/or amplitude of possible conformations. These data suggest that the variability observed in the GlcNS,6S-(1→4)-IdoA2S $\psi$ angle among different experimentally determined structures is higher in IdoA2S skew-boat-containing oligosaccharides due to the capability of these pyranose conformations to fit a broader set of binding pockets when compared to the IdoA2S chairs containing compounds. Moreover, the shape and size of the minimum-energy regions, as described in the relaxed contour plots, may be considered as an estimation of a disaccharide plasticity, which would be explored differently by distinct environments, as aqueous solutions, membranes and target receptors.

Additionally, the heparin-relaxed maps (Fig. 2) show a variable amount of minimum-energy conformations, varying from one main conformation (GlcNS,6S-(1→4)-IdoA2S linkage with IdoA2S as $^2S_O$, Fig. 2B) to at least four main conformations (IdoA2S-(1→4)-GlcNS,6S linkage with IdoA2S as $^2S_O$, Fig. 2F). Although these maps do not represent the lowest energy of all possible pendent group orientations at each point of the $\phi$, $\psi$ conformational space, they do describe the conformational preference of heparin according to NMR[14] (Table 1). Additionally, most methods for describing oligosaccharide conformations through exploring $\phi$, $\psi$ conformational space have limitations in describing solvent effects, mainly its explicit influence over solute molecules, resulting in vacuum minimum-energy conformations that may not be retained in aqueous solutions. Therefore, to include the influence of water molecules on heparin geometry we further refined the

**Table 1.** Geometry of heparin glycosidic linkage around residues IdoA2S and GlcNS,6S considering different mediums and uronic acid conformations ($^1C_4$ and $^2S_O$)

| IdoA form | Source | Dihedral angles from heparin analogues (°)[a] | | | | | | | |
|---|---|---|---|---|---|---|---|---|---|
| | | IdoA2S(1→4) GlcNS,6S | | GlcNS,6S(1→4) IdoA2S | | IdoA2S(1→4) GlcNS | | GlcNAc,6S(1→4) IdoA2S | |
| | | $\phi$ | $\psi$ | $\phi$ | $\psi$ | $\phi$ | $\psi$ | $\phi$ | $\psi$ |
| $^1C_4$ | Experimental average[b] | −69 ± 17 | −118 ± 31 | 73 ± 16 | −151 ± 15 | —[f] | — | — | — |
| | NMR[c] | −77 | −110 | 79 | −150 | — | — | — | — |
| | Contour plot[d] | −121 | −150 | 91 | −120 | | | | |
| | Disaccharide MD | −113 ± 28 | −142 ± 31 | 77 ± 14 | −150 ± 11 | −117 ± 32 | −136 ± 26 | 79 ± 18 | −147 ± 12 |
| | Decasaccharide MD[e] | −124 ± 18 | −145 ± 11 | 90 ± 12 | −141 ± 11 | — | — | — | — |
| $^2S_O$ | Experimental average[b] | −69 ± 15 | −123 ± 23 | 76 ± 18 | −147 ± 27 | — | — | — | — |
| | NMR[c] | −55 | −107 | 109 | −158 | — | — | — | — |
| | Contour plot[d] | −90 | −145 | 88 | −121 | | | | |
| | Disaccharide MD | −84 ± 39 | −126 ± 32 | 94 ± 20 | −96 ± 17 | −95 ± 18 | −127 ± 17 | 88 ± 23 | −109 ± 27 |
| | Decasaccharide MD[e] | −75 ± 11 | −117 ± 11 | 97 ± 14 | −125 ± 15 | — | — | — | — |

[a] See Section 2 for details.

[b] Data adapted from Ref. 31, with addition of heparin conformations described at PDB ID 2ERM.[12] Twenty-six (26) values were used to obtain a $^2S_O$ average at the IdoA2S(1→4)GlcNS linkage and thirty (30) values to obtain $^2S_O$ average at the GlcNS(1→4)IdoA2S linkage. Twenty-eight (28) values were used to obtain a $^1C_4$ average at the IdoA2S(1→4)GlcNS linkage, while forty-four (44) values to obtain $^2S_O$ average at the GlcNS(1→4)IdoA2S linkage. The GlcNS sulfation pattern was omitted in order to give a broad perspective of heparin linkage flexibilities.

[c] Data from Ref. 14.

[d] The minimum-energy conformation closest to the experimental values.

[e] Data from Ref. 15.

[f] Non-available or non-calculated.

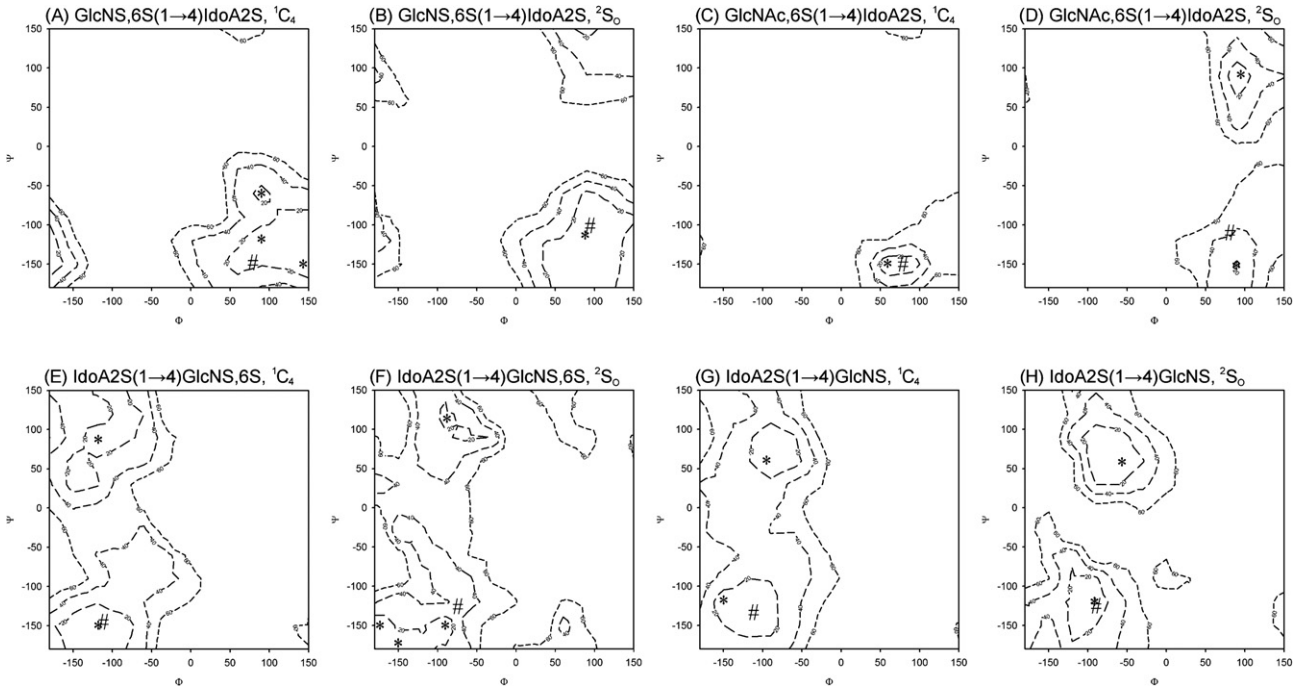


**Figure 2.** Contour plots of heparin glycosidic linkages as a function on IdoA2S conformation. The GlcNS,6S-(1→4)-IdoA2S linkage is presented with IdoA2S in $^1C_4$ conformation (A) and $^2S_O$ conformation (B). The GlcNAc,6S-(1→4)-IdoA2S linkage is presented with IdoA2S in $^1C_4$ conformation (C) and $^2S_O$ conformation (D). The IdoA2S-(1→4)-GlcNS,6S linkage is also presented with IdoA2S in $^1C_4$ conformation (E) and $^2S_O$ conformation (F). The IdoA2S-(1→4)-GlcNS linkage is described with IdoA2S in $^1C_4$ conformation (G) and $^2S_O$ conformation (H). Contour levels are shown at every 20 kJ mol$^{-1}$ from 20 to 60 kJ mol$^{-1}$. Asterisks (∗) indicate the input minimum-energy conformations for MD refinement, and sharps (#) indicate the final conformations after 200 ns.

main identified minimum-energy conformations, indicated in Figure 2 by asterisks, through a series of 0.2 μs MD simulations.

As a consequence of MD simulations in explicit solvent, the multiple minimum-energy conformations from each glycosidic linkage converged to a single conformational state. In some of the evaluated angles, the values obtained in MD simulations are very close to one of the minimum-energy conformations described in the contour plots, as seen in Figure 2B and C, indicating that the solvent is not capable of further stabilizing these minimum-energy conformations. On the other hand, the angles presented in Figure 2D and F present a relevant contribution of solvent to stabilization of the glycosidic linkage geometry, as the MD obtained conformation populates a higher energy region on the contour plot when compared to the vacuum one. Additionally, the adequacy in the use of MD simulations to refine minimum-energy conformations obtained from contour plots can be ascertained through observation of great interconversion paths during the simulations, as observed for IdoA2S-(1→4)-GlcNS,6S (Fig. 2E and F), IdoA2S-(1→4)-GlcNS (Fig. 2G and H), and GlcNAc-(1→4)-IdoA2S (Fig. 2D) linkages, originating values in agreement with the previous results from heparin MD[15,20] and NMR,[14] as shown in Table 1 and Supplementary data. The fluctuation of the most prevalent dihedral angles is presented in Figure 3.

The precise elucidation of the forces governing the conformational preferences mentioned above can be determined by the predominant interactions between monosaccharide units in each glycosidic linkage, mainly hydrogen-bond interactions. In this context, we proceeded to evaluate the intramolecular hydrogen bonds observed to occur in the MD simulations for these heparin disaccharides. Depending on the disaccharide, up to 54 possible interactions may be observed, totalizing 412 interactions for all the simulated systems. These data, including fluctuation and distribution of hydrogen-bond distance and angle, are included as Supplementary data. Nevertheless, most disaccharides present from two to four hydrogen-bond interactions, with different prevalences and strengths, that is, agreement between distance and angle cut-offs to its reference values. One of these interactions always involved the oxygen atom from the glycosidic linkage as the acceptor group. Because this interaction occurs in both the $^2S_O$ and $^1C_4$ conformations of IdoA2S, it cannot be related to properties specific to hexopyranose conformation. On the other hand, one main interaction, including donor and acceptor groups from both neighbor monosaccharide residues, was also observed as a high prevalent interaction in the time scale of the performed simulation. These results are summarized in Figure 4.

Regarding the GlcNS,6S-(1→4)-IdoA2S linkage, different hydrogen-bond interactions are established as a

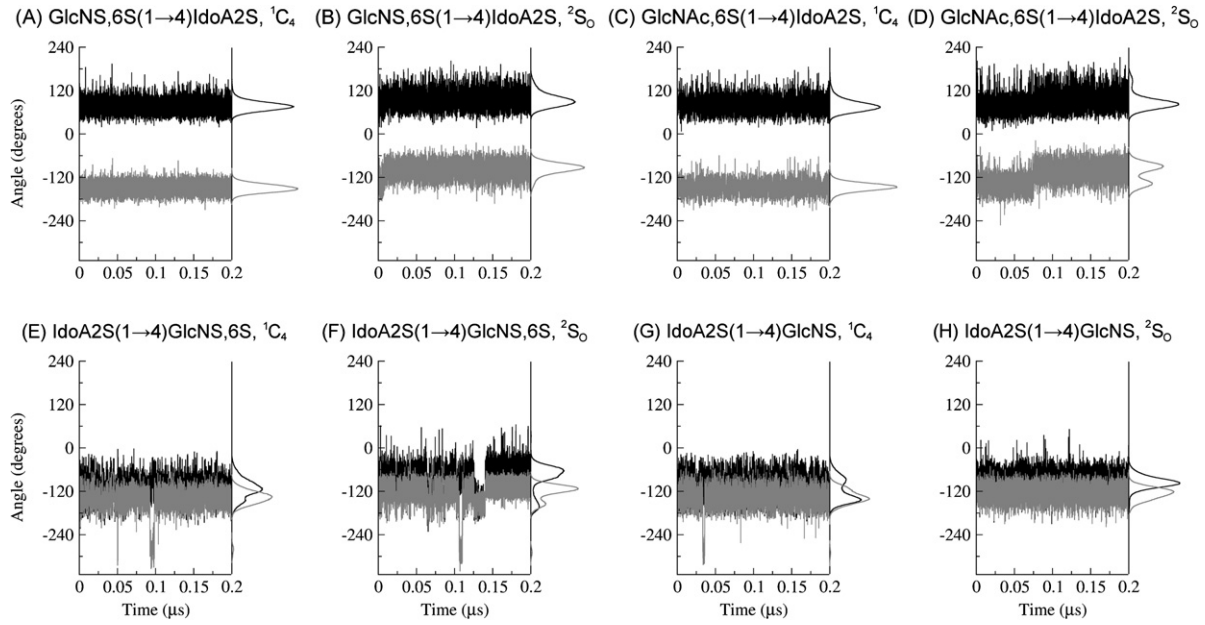


**Figure 3.** Fluctuation and distribution of the $\phi$ (black) and $\psi$ (gray) dihedral angles associated with heparin disaccharides formed by GlcNS,6S, GlcNAc,6S, GlcNS, and IdoA2S, as a function of IdoA pyranose conformation: $^1C_4$ (A, C, E, and G) and $^2S_O$ (B, D, F, and H).

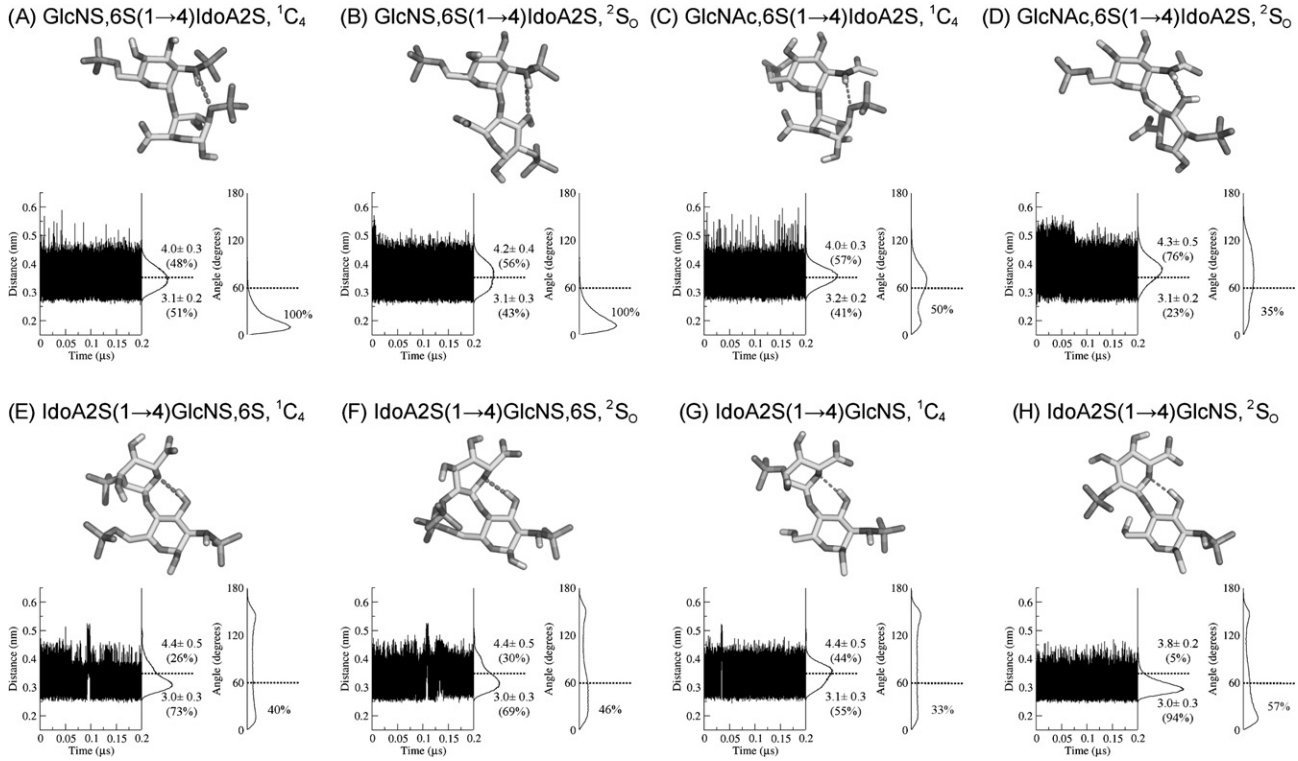


**Figure 4.** Representation of the intramolecular hydrogen-bond interactions observed to occur in heparin disaccharides formed by GlcNS,6S, GlcNAc,6S, GlcNS, and IdoA2S, as a function of IdoA pyranose conformation: $^1C_4$ (A, C, E, and G) and $^2S_O$ (B, D, F, and H). Each interaction is represented with a dotted line. The fluctuation and distribution of the distance associated with these interactions are also presented, together with average and prevalence values (%) for each conformer population.

consequence of IdoA geometry, as the $^1C_4$ conformation promotes a hydrogen bond between the NH group from sulfonamide attached at GlcNS,6S C-2 and the oxygen atom from the sulfate group attached at C-2 of IdoA2S (Fig. 4A). Conversely, in the $^2S_O$ conformation the hydroxyl group at IdoA2S C-3 is exposed and becomes the acceptor of a hydrogen bond in the place of C-2 sulfate group (Fig. 4B). The torsion of the IdoA2S

pyranose ring from a chair to a skew-boat form promotes a small reduction in the amount of intramolecular hydrogen bonds, from 51% in the $^{1}C_4$ chair to 43% in the $^{2}S_O$ skew-boat (Fig. 4A and B). The global quantitation of the inter-residue interactions agrees with these modifications in the prevalence and strength (i.e., characteristics of the acceptor group at IdoA2S, changed from a C-2 sulfate to a C-3 hydroxyl) of this hydrogen bond, resulting in $-0.5 \pm 9.9$ kJ/mol in the IdoA2S chair conformation and $3.4 \pm 7.2$ kJ/mol in the IdoA2S skew-boat form ($p < 0.05$).

Another hydrogen bond is observed around the IdoA2S-(1→4)-GlcNS,6S linkage, taking place between GlcNS,6S hydroxyl group at C-3 and the ether oxygen atom from IdoA2S (Fig. 4E and F). In this linkage, different from the GlcNS,6S-(1→4)-IdoA2S disaccharides, the acceptor of the hydrogen bond is independent of the IdoA2S ring conformation. Again, there is a progressive tendency to reduce the amount of this interaction in $^{2}S_O$-containing IdoA2S sequences. However, possibly due to the lower polarity of the acceptor group and to the weaker hydrogen-bond angle values in the simulations, this interaction does not contribute significantly to further stabilization of this glycosidic linkage, which presents an inter-residue interaction energy of $15.2 \pm 11.6$ kJ/mol in the IdoA2S chair conformation and $19.1 \pm 8.4$ kJ/mol in the IdoA2S skew-boat form ($p < 0.05$).

### 3.2. Dynamics of linkages between IdoA2S, GlcNAc,6S, and GlcNS

It is known that the substitution pattern on heparin monosaccharide residues can modify the conformational equilibrium adopted by IdoA.[21,35] For example, when attached to GlcNS,6S residues, IdoA2S lies approximately 40% at the $^{2}S_O$ form and 60% at the $^{1}C_4$ chair.[4] However, through acetylation of the preceding GlcNS,6S residue and sulfate group removal at C-6 of the succeeding GlcNS, IdoA2S appears to no longer populate skew-boat conformational states.[21] Considering that IdoA2S monosaccharides in solution are mainly $^{1}C_4$ chairs, we analyzed the conformation adopted in solution by compound **2** in comparison to the behavior of compound **1** in the same conditions.

As a general feature, chemical modifications in **2** compared to **1** promote an increase in rigidity of the glycosidic linkages, IdoA2S-(1→4)-GlcNS,6S versus IdoA2S-(1→4)-GlcNS and GlcNS,6S-(1→4)-IdoA2S versus GlcNAc,6S-(1→4)-IdoA2S (Fig. 2 and Table 1), with no apparent connection to IdoA2S conformation. Additionally, the interconversion between the global minimum in Figure 2D (GlcNS,6S-(1→4)-IdoA2S) and Figure 2H (IdoA2S-(1→4)-GlcNS) to a local minima suggests an important role of the solvent on conformational stabilization of this derivative, as is also observed for the IdoA2S-(1→4)-GlcNS,6S (Fig. 2F) and depicted in Supplementary data.

From MD simulations of each minimum-energy conformation retrieved from the relaxed contour plots, the profile of intramolecular hydrogen-bond interactions observed in **2** was obtained and compared to those discussed above for **1** (Fig. 4). Considering disaccharide units containing IdoA2S in a $^{1}C_4$ chair, the acetylation of the sulfonamide group at C-2 does not interfere with the donation of a hydrogen-bond distance to IdoA C-2 sulfate group (Fig. 4A and C). However, acetylation considerably reduces the prevalence of the hydrogen bond with IdoA C-3 hydroxyl group (Fig. 4B and D). In fact, this behavior may be illustrated by the inter-residue interaction energy for heparin analogue **2**, of $-16.9 \pm 8.0$ kJ/mol in the IdoA2S chair conformation and $4.9 \pm 6.4$ kJ/mol in the IdoA2S skew-boat form ($p < 0.05$). On the other hand, and similar to the behavior observed for heparin analogue **1**, the hydrogen bond between GlcNS C-3 hydroxyl group and the endocyclic oxygen atom from IdoA2S (Fig. 4G and H) is weaker; $20.9 \pm 7.4$ kJ/mol in the IdoA2S chair conformation and $11.7 \pm 6.1$ kJ/mol in the IdoA2S skew-boat form ($p < 0.05$). As may be observed, the inter-residue interactions occurring in different parts of heparin show different contributions to stabilization of a skew-boat conformation, with a predominant contribution of the GlcNS,6S-(1→4)-IdoA2S (or GlcNAc,6S-(1→4)-IdoA2S) over the IdoA2S-(1→4)-GlcNS,6S (or IdoA2S-(1→4)-GlcNS).

### 3.3. Role of solvation

The data obtained from MD suggest an important role of intra-chain hydrogen bonds for stabilization of IdoA2S conformation. As shown in Figures 3 and 4, these interactions present a highly flexible pattern, dependent on the explicit presence of water molecules. Still, it most likely results in a distinct influence of heparin on the surrounding solvent as being due to the IdoA2S conformational change. Because the previous evidence supports individual carbohydrate–water interactions as being able to determine carbohydrate conformation and functionality,[36] we analyzed both radial distribution functions and water residence times around the polar groups in **1** and **2**, as presented in Figure 5 and Table 2, respectively.

The hydrogen-bond groups of GlcN residues in both **1** and **2** did not show differences in solvation as being due to IdoA2S conformational modification (Supplementary data). The IdoA2S residue, on the other hand, has changes in its hydration shells upon transition between $^{2}S_O$ and $^{1}C_4$ conformations (Fig. 5—only the groups with differences in solvation between the two forms of IdoA2S are presented, while the remaining groups are presented in the Supplementary data). As a general

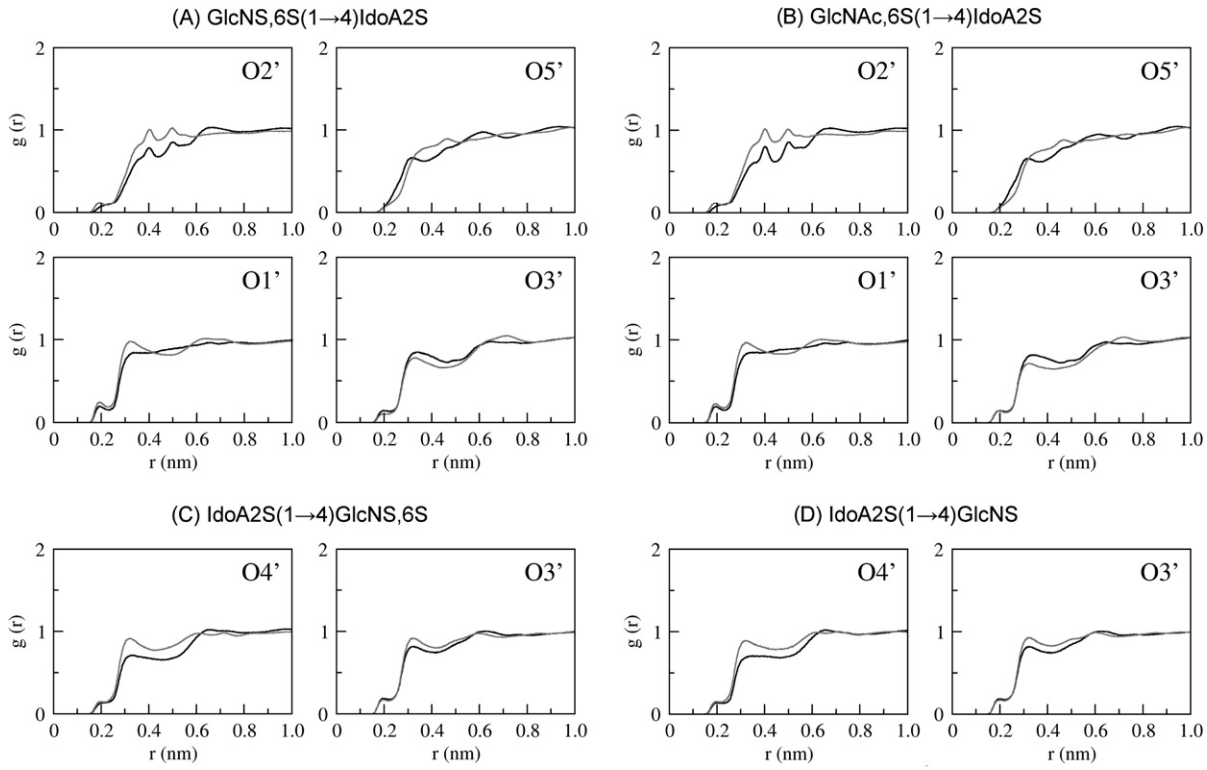


**Figure 5.** Radial distribution functions of water molecules around IdoA2S polar atoms on heparin disaccharides formed by GlcNS,6S and IdoA2S (A and C), GlcNAc,6S, GlcNS, and IdoA2S (B and D). Accordingly, the pattern of each disaccharide solvation as a function of IdoA2S conformation is presented ($^1C_4$ as black lines and $^2S_O$ as gray lines). A description of all polar groups of compounds **1** and **2** can be found in Supplementary data.

feature, the skew-boat form appears to be more solvated than the chair conformation, with the exception of the IdoA2S 3-OH group in GlcNS,6S-(1→4)-IdoA2S and GlcNAc,6S-(1→4)-IdoA2S linkages. In these cases this group acts as an intramolecular hydrogen-bond acceptor with, respectively, 2-sulfonamide and 2-acetamide groups, in both **1** and **2** containing a $^2S_O$ IdoA2S, which appears to hinder its solvent accessibility.

Moreover, the degree of exposure to solvent also appears to correlate with IdoA2S conformational preference. As a general feature, the skew-boat conformation in **1** is more tightly bound to water molecules than in **2** (differences from 2 to 3 ps, approximately, with $p \leqslant 0.001$), as observed for the oxygen atoms of the IdoA 2-sulfate group (Table 2), mainly around GlcNS,6S-(1→4)-IdoA2S and GlcNAc,6S-(1→4)-IdoA2S linkages. On the other hand, the differences in water residence times for **1** and **2** around the 2-sulfate group in the IdoA2S-(1→4)-GlcNS,6S and IdoA2S-(1→4)-GlcNS linkages appear to be similarly influenced by the additional sulfate group on GlcN residue in **1**, and not related to conformational changes in IdoA residue.

### 3.4. IdoA2S behavior in heparin oligosaccharides

Several factors may guide the conformational preference of IdoA in different environments, for example, solutions, complexation to target proteins, oligosaccharide size and composition. At the molecular level, all these modifications in heparin surroundings can be expressed through different contributions of forces, as the thermodynamic conformational preference of IdoA monosaccharide, inter-residue interactions, solute–solvent interactions, and ligand–receptor interactions. Together with the adequate conformational sampling, the precise evaluation through molecular modeling techniques of all these factors should allow an accurate reproduction of the polysaccharide conformation, both at the pyranose ring and glycosidic linkage levels.

Early force field calculations on heparin oligosaccharides had pointed out that the 3-*O*-sulfo group at the preceding GlcNS residue promotes a stabilization of the $^2S_O$ conformation of IdoA.[4] Additionally, NMR data indicated that IdoA conformation is mainly affected by the substituents at positions $2^{21}$ and $3^{11}$ of GlcNS. However, the driving forces and/or interactions responsible for these stabilization and conformational preferences are uncertain. Considering the expected influence of the solvent molecules in this equilibrium as well as its dynamic nature, one of the strategies best suited to investigate such conformational events can be found in MD.[37]

In fact, MD simulations had previously been successfully applied in the description of the skew-boat pseudo-

**Table 2.** Water residence time around polar atoms of residues IdoA2S and GlcNS, considering different uronic acid conformations ($^1C_4$ and $^2S_O$)

| Residue | Atom | Water residence time on heparin analogues (ps)* | | | | | | | |
|---|---|---|---|---|---|---|---|---|---|
| | | (**1**) IdoA2S(1→4)GlcNS,6S | | (**2**) IdoA2S(1→4)GlcNS | | (**1**) GlcNS,6S(1→4)IdoA2S | | (**2**) GlcNAc,6S(1→4)IdoA2S | |
| | | $^1C_4$ | $^2S_O$ | $^1C_4$ | $^2S_O$ | $^1C_4$ | $^2S_O$ | $^1C_4$ | $^2S_O$ |
| GlcNS | O6 (hydroxyl) | — | — | 11.8 ± 0.5 | 11.3 ± 0.9 | — | — | — | — |
| | O6 (sulfate) | **5.8 ± 0.6**[a] | **8.4 ± 0.5**[a] | — | — | **6.6 ± 0.3**[b] | **6.6 ± 0.4**[c] | **5.8 ± 0.4**[b] | **5.7 ± 0.2**[c] |
| | O6A | 17.1 ± 0.9 | 17.3 ± 2.3 | — | — | **15.5 ± 0.5**[b] | 15.5 ± 0.7 | **14.6 ± 0.5**[b] | 14.7 ± 0.7 |
| | O6B | 17.5 ± 1.6 | 17.6 ± 1.6 | — | — | 15.6 ± 1.1 | 15.4 ± 1.0 | 14.7 ± 0.9 | 15.2 ± 1.0 |
| | O6C | 17.5 ± 1.1 | 17.5 ± 2.0 | — | — | 15.2 ± 0.8 | 15.2 ± 0.2 | 14.8 ± 0.7 | 15.3 ± 0.6 |
| | O5 | 7.9 ± 0.8 | **8.8 ± 0.8**[c] | 7.0 ± 0.3 | **7.0 ± 0.6**[c] | **11.3 ± 0.8**[a,b] | **9.9 ± 0.7**[a] | **9.8 ± 0.5**[b] | 9.5 ± 1.3 |
| | O1 | **10.0 ± 0.6**[b] | **10.7 ± 0.6**[c] | **6.4 ± 0.6**[b] | **6.7 ± 0.4**[c] | — | — | — | — |
| | O4 | — | — | — | — | 10.0 ± 0.5 | 9.5 ± 0.6 | 9.5 ± 0.5 | 9.2 ± 0.8 |
| | O3 | 13.5 ± 1.1 | 14.1 ± 1.6 | 12.4 ± 0.8 | 13.0 ± 0.7 | **10.8 ± 0.7**[a,b] | **9.6 ± 0.4**[a,c] | **9.1 ± 0.4**[a,b] | **8.2 ± 0.5**[a,c] |
| | N2 | 5.4 ± 0.5 | **5.5 ± 0.3**[c] | 4.9 ± 0.4 | **4.9 ± 0.3**[c] | **8.5 ± 0.6**[a,b] | **5.6 ± 0.2**[a] | **9.6 ± 0.6**[a,b] | **5.7 ± 0.4**[a] |
| | O2 | — | — | — | — | — | — | 9.7 ± 0.7 | 9.8 ± 0.9 |
| | O2A | 19.0 ± 1.3 | 21.7 ± 2.4 | 20.4 ± 1.4 | 19.6 ± 1.9 | 24.9 ± 2.0 | 22.8 ± 3.4 | — | — |
| | O2B | 19.8 ± 1.6 | 19.7 ± 1.0 | 20.0 ± 1.4 | 20.5 ± 1.3 | **27.2 ± 1.9**[a] | **23.3 ± 2.6**[a] | — | — |
| | O2C | 20.5 ± 1.2 | 19.6 ± 2.8 | 20.1 ± 1.2 | 19.8 ± 2.2 | 24.7 ± 2.7 | 25.1 ± 3.2 | — | — |
| IdoA | OGL | 10.9 ± 1.8 | 12.7 ± 1.8 | **8.7 ± 0.3**[a] | **12.5 ± 0.6**[a] | **31.9 ± 1.8**[a] | **14.0 ± 1.0**[a] | **33.0 ± 1.9**[a] | **13.9 ± 1.1**[a] |
| | O6A′ | 14.5 ± 1.3 | 16.7 ± 2.0 | **14.1 ± 0.4**[a] | **18.6 ± 0.5**[a] | 21.1 ± 1.1 | 20.6 ± 0.7 | 20.7 ± 1.7 | 20.5 ± 1.6 |
| | O6B′ | 14.7 ± 1.5 | 16.8 ± 1.8 | **14.0 ± 0.7**[a] | **18.8 ± 1.1**[a] | 20.9 ± 1.1 | 20.6 ± 1.1 | 21.0 ± 0.7 | 20.7 ± 1.1 |
| | O5′ | 10.9 ± 0.8 | **11.9 ± 2.0**[c] | **10.2 ± 0.7**[a] | **7.3 ± 0.4**[a,c] | **17.0 ± 1.0**[a] | **8.3 ± 0.5**[a] | **18.1 ± 1.2**[a] | **8.4 ± 1.2**[a] |
| | O1′ | — | — | — | — | **8.1 ± 0.6**[a] | **10.0 ± 0.5**[a] | **8.0 ± 0.6**[a] | **9.4 ± 0.5**[a] |
| | O4′ | 9.9 ± 0.6 | 9.0 ± 0.5 | **9.5 ± 0.5**[a] | **8.1 ± 0.5**[a] | — | — | — | — |
| | O2′ | **6.4 ± 0.4**[a] | **9.4 ± 1.4**[a,c] | **6.2 ± 0.4**[a] | **7.1 ± 0.4**[a,c] | **19.0 ± 1.1**[a] | **6.7 ± 0.3**[a] | **20.4 ± 1.1**[a] | **6.5 ± 0.4**[a] |
| | O2A′ | **19.9 ± 1.1**[b] | **20.4 ± 0.7**[c] | **17.6 ± 1.3**[b] | **17.1 ± 0.9**[c] | **19.8 ± 1.1**[a] | **16.4 ± 1.0**[a,c] | **19.1 ± 1.0**[a] | **14.4 ± 1.3**[a,c] |
| | O2B′ | **20.2 ± 1.9**[b] | **20.4 ± 1.3**[c] | **17.5 ± 1.0**[b] | **17.4 ± 1.0**[c] | **20.1 ± 1.2**[a] | **16.7 ± 0.9**[a,c] | **19.0 ± 1.1**[a] | **14.9 ± 0.7**[a,c] |
| | O2C′ | **20.1 ± 1.3**[b] | **20.2 ± 1.6**[c] | **17.7 ± 0.8**[b] | **17.5 ± 1.4**[c] | **20.2 ± 1.2**[a] | **16.0 ± 0.7**[a] | **18.8 ± 0.9**[a] | **15.0 ± 1.0**[a] |
| | O3′ | **12.3 ± 1.0**[a,b] | **10.2 ± 0.7**[a] | **9.4 ± 0.4**[b] | 9.6 ± 0.4 | **10.1 ± 0.3**[a,b] | **12.5 ± 0.7**[a,c] | **8.7 ± 0.5**[a,b] | **11.0 ± 0.8**[a,c] |

* The values presenting some degree of statistical significance when compared to the other values are marked as bold.
[a] $p \leqslant 0.001$, comparing a same disaccharide with IdoA2S in $^1C_4$ and $^2S_O$ conformations.
[b] $p \leqslant 0.001$, comparing disaccharides in compounds **1** and **2** with IdoA2S in $^1C_4$ conformation.
[c] $p \leqslant 0.001$, comparing disaccharides in compounds **1** and **2** with IdoA2S in $^2S_O$ conformation.

rotational ensemble of IdoA in heparin.[38] Unfortunately, the description of the chair–skew-boat interconversion was not studied by the authors due to the timescale associated with such a process.[5,38] Still, this work indicates that MD techniques are indeed capable of describing solute–solvent interaction in heparin dynamics, an assumption also supported by works of our group using force fields as GROMACS and GROMOS96.[15,20] Additionally, the use of MD simulations in a quantitative reproduction of heparin–AT interaction was also accessed.[9] On the other hand, recent work has been able to mimic the conformational preference of IdoA monosaccharides.[7] However, the contribution of inter-residue interactions to these unusual conformational preferences has not been elucidated, despite its evident relevance. It has been known for more than 20 years that the oligosaccharide sequence, size and composition greatly contribute to the form adopted by the IdoA pyranose ring.[4]

It should be noted that the hydrogen-bond interactions observed to occur in glycosidic linkages may represent driving forces for the modification in IdoA2S conformational preferences through modifications in the composition of oligosaccharide sequences. Considering the above-mentioned inter-residue interaction energies for heparin analogue **1**, it can be evidenced that a trisaccharide composed of GlcNS,6S–IdoA2S and IdoA2S-GlcNS,6S would present a total inter-residue interaction of 14.7 ± 15.0 kJ/mol with an IdoA2S residue in a $^1C_4$ conformation and 22.5 ± 11.1 kJ/mol with an IdoA2S residue in a $^2S_O$ conformation. As can be observed, there is a higher energy penalty in skew-boat-containing oligosaccharides compared to those presenting a chair IdoA. As shown in Figure 4, this appears to be due to a small decrease in inter-residue interactions that occur when the uronic acids present a skewed conformation.

In the case of heparin analogue **2**, a trisaccharide composed by GlcNAc,6S–IdoA2S and IdoA2S–GlcNS would present a total inter-residue interaction of 3.1 ± 10.9 kJ/mol with an IdoA2S residue in a $^1C_4$ conformation and 16.6 ± 8.8 kJ/mol with an IdoA2S residue in a $^2S_O$ conformation. Again, the skewed conformation destabilizes the oligosaccharide conformation. In fact, this destabilization in analogue **2** is almost twice (13.5 ± 14.0 kJ/mol) that observed in heparinoid **1** (7.8 ± 18.7 kJ/mol), which may be related to the greater prevalence of $^1C_4$ conformation in IdoA

in **2** ($p \leqslant 0.001$). These data are in agreement with the previous data demonstrating the importance of inter-residue hydrogen bonds on the determination of IdoA2S conformation, based on B3LYP/6-311++G** calculations.[39] Additionally, although previous works based on quantum-mechanical calculations have pointed to the importance of covalently bound counter ions, the MD data obtained in this work, covering a time scale of 0.2 μs, suggest that this should not be a general property associated with all hexopyranose rings in heparin, as can be observed from a comparison between disaccharide MD and NMR-derived data (Table 1). Indeed, the obtained data suggest that, probably, the heparin dihedral angle most susceptible to the influence of ions should be the $\psi$ angle from GlcNS,6S-(1→4)-IdoA2S glycosidic linkage. In this process of conformational modification, it became clear that solute and solvent exert mutual influences, with the solvent further stabilizing the glycosidic linkage geometry (Figs. 2 and 3) and the IdoA2S modifying its hydration shells.

## 4. Conclusions

Several reports have pointed to the importance of IdoA2S solution conformational equilibrium to the biological properties of heparin. Structurally, these predictions point to conformer-specific interactions between heparin and its target proteins, such as AT. Additionally, modifications in heparin sequence are known to contribute both to its biological properties and to IdoA2S conformation, whereas the relation between the two properties is a complex task. Nevertheless, there are potential implications to the design of new heparin synthetic analogues.

The use of molecular modeling techniques can be expected to greatly contribute in the elucidation of the relation between heparin structure and biological properties. Unfortunately, glycosaminoglycan modeling has been methodologically limited in comparison to studies with other biomacromolecules, such as proteins and nucleic acids. This is due, for example, to difficulties in parameterization and in validation of the obtained conformations with experimental data. In this context, the current work analyzes the conformational equilibrium of IdoA2S in oligosaccharide sequences as a function of solvent and polysaccharide sequence composition. The obtained data point to the role of intra-chain hydrogen bonds as a possible driving force for a chair to skew-boat conformational modification in IdoA2S from its monosaccharide form to a polysaccharide containing sequence, which in turn appears to influence the surrounding solvent structure and dynamics. Thus, different heparin compositions would be able to modify these hydrogen-bond interactions and so the IdoA2S conformation in biological conditions. As both $^{1}C_{4}$ and $^{2}S_{O}$ conformations of IdoA2S are capable of being retained when complexed with its target proteins, a significant contribution from upcoming studies using molecular modeling techniques can be expected in the search for elucidation of the roles of receptor specificity or solution conformational predominance in the formation of these carbohydrate–protein complexes.

## Acknowledgments

The authors thank M.Sc. F.S. Poletto (PPGCF-UFRGS, Porto Alegre) for the statistical analysis. This work was supported by the Conselho Nacional de Desenvolvimento Científico e Tecnológico (CNPq #420015/05-1 and #472174/2007-0), MCT, the Coordenação de Aperfeiçoamento de Pessoal de Nível Superior (CAPES), MEC, Brasília, DF, Brazil.

## Supplementary data

Supplementary data associated with this article can be found, in the online version, at doi:10.1016/j.carres.2008.04.016.

## References

1. Nader, H. B.; Pinhal, M. A. S.; Baú, E. C.; Castro, R. A. B.; Medeiros, G. F.; Chavante, S. F.; Leite, E. L.; Trindade, E. S.; Shinjo, S. K.; Rocha, H. A.; Tersariol, I. L. S.; Mendes, A.; Dietrich, C. P. *Braz. J. Med. Biol. Res.* **2001**, *34*, 699–709.
2. Silva, M. E.; Dietrich, C. P. *J. Biol. Chem.* **1975**, *250*, 6841–6846.
3. Gettins, P. G. W. *Chem. Rev.* **2002**, *102*, 4751–4803.
4. Ferro, D. R.; Provasoli, A.; Ragazzi, M.; Torri, G.; Casu, B.; Gatti, G.; Jacquinet, J. C.; Sinay, P.; Petitou, M.; Choay, J. *J. Am. Chem. Soc.* **1986**, *108*, 6773–6778.
5. Mulloy, B.; Forster, M. *J. Glycobiol.* **2000**, *10*, 1147–1156.
6. Casu, B.; Choay, J.; Ferro, D. R.; Gatti, G.; Jacquinet, J. C.; Petitou, M.; Provasoli, A.; Ragazzi, M.; Sinay, P.; Torri, G. *Nature* **1986**, *322*, 215–216.
7. Hricovíni, M. *Carbohydr. Res.* **2006**, *341*, 2575–2580.
8. Remko, M.; von der Lieth, C.-W. *J. Chem. Inf. Model.* **2006**, *46*, 1194–1200.
9. Verli, H.; Guimarães, J. A. *J. Mol. Graph. Model.* **2005**, *24*, 203–212.
10. Jin, L.; Abrahams, J. P.; Skinner, R.; Petitou, M.; Pike, R. N.; Carrell, R. W. *Proc. Natl. Acad. Sci. U.S.A.* **1997**, *94*, 14683–14688.
11. van Boeckel, C. A. A.; Beetz, T.; van Aelst, S. F. *Tetrahedron Lett.* **1988**, *29*, 803–806.
12. Canales, A.; Angulo, J.; Ojeda, R.; Bruix, M.; Fayos, R.; Lozano, R.; Giménez-Gallego, G.; Martín-Lomas, M.; Nieto, P. M.; Jiménez-Barbero, J. *J. Am. Chem. Soc.* **2005**, *127*, 5578–5779.
13. Canales, A.; Lozano, R.; López-Méndez, B.; Angulo, J.; Ojeda, R.; Nieto, P. M.; Martín-Lomas, M.; Giménez-Gallego, G.; Jiménez-Barbero, J. *FEBS J.* **2006**, *273*, 4716–4727.

14. Mulloy, B.; Forster, M. J.; Jones, C.; Davies, D. B. *Biochem. J.* **1993**, *293*, 849–858.
15. Verli, H.; Guimarães, J. A. *Carbohydr. Res.* **2004**, *339*, 281–290.
16. IUPAC–IUB Commission on Biochemical Nomenclature, *Pure Appl. Chem.* **1996**, *68*, 1919–2008.
17. Schuettelkopf, A. W.; van Aalten, D. M. F. *Acta Crystallogr., Sect. D* **2004**, *60*, 1355–1363.
18. Schaftenaar, G. MOLDEN. CAOS/CAMM Center, University of Nijmegen, Toernooiveld 1, 6525 ED NIJMEGEN, The Netherlands, 1997.
19. van der Spoel, D.; Lindahl, E.; Hess, B.; Groenhof, G.; Mark, A. E.; Berendsen, H. J. C. *J. Comput. Chem.* **2005**, *26*, 1701–1718.
20. Becker, C. F.; Guimarães, J. A.; Verli, H. *Carbohydr. Res.* **2005**, *340*, 1499–1507.
21. van Boeckel, C. A. A.; Aelst, S. F.; Wagenaars, G. N.; Mellema, J.-R.; Paulsen, H.; Peters, T.; Pollex, A.; Sinwell, V. *Recl. Trav. Chim. Pays-Bas* **1987**, *106*, 19–29.
22. de Groot, B. L.; Grubmüller, H. *Science* **2001**, *294*, 2353–2357.
23. Hess, B.; Bekker, H.; Berendsen, H. J. C.; Fraaije, J. G. E. M. *J. Comput. Chem.* **1997**, *18*, 1463–1472.
24. Darden, T.; York, D.; Pedersen, L. *J. Chem. Phys.* **1992**, *98*, 10089–10092.
25. Luzar, A.; Chandler, D. *Nature* **1996**, *379*, 55–57.
26. DiGabriele, A. D.; Lax, I.; Chen, D. I.; Svahn, C. M.; Jaye, M.; Schlessinger, J.; Hendrickson, W. A. *Nature* **1998**, *393*, 812–817.
27. Schlessinger, J.; Plotnikov, A. N.; Ibrahimi, O. A.; Eliseenkova, A. V.; Yeh, B. K.; Yayon, A.; Linhardt, R. J.; Mohammadi, M. *Mol Cell.* **2000**, *6*, 743–750.
28. Swaminathan, G. J.; Myszka, D. G.; Katsamba, P. S.; Ohnuki, L. E.; Gleich, G. J.; Acharya, K. R. *Biochemistry* **2005**, *44*, 14152–14158.
29. Capila, I.; Hernaiz, M. J.; Mo, Y. D.; Mealy, T. R.; Campos, B.; Dedman, J. R.; Linhardt, R. J.; Seaton, B. A. *Structure* **2001**, *9*, 57–64.
30. Lietha, D.; Chirgadze, D. Y.; Mulloy, B.; Blundell, T. L.; Gherardi, E. *Embo J.* **2001**, *20*, 5543–5555.
31. Pellegrini, L.; Burke, D. F.; von Delft, F.; Mulloy, B.; Blundell, T. L. *Nature* **2000**, *407*, 1029–1034.
32. Guerrini, M.; Guglieri, S.; Beccati, D.; Torri, G.; Viskov, C.; Mourrier, P. *Biochem. J.* **2006**, *399*, 191–198.
33. Ganesh, V. K.; Smith, S. A.; Kotwal, G. J.; Murthy, K. H. M. *Proc. Natl. Acad. Sci. U.S.A.* **2004**, *101*, 8924–8929.
34. Verli, H.; Guimarães, J. A. Molecular Modeling in the Assessment of Glycosaminoglycans Structure and Function. In *Insights into Carbohydrate Structure and Biological Function*; Verli, H., Ed.; Transworld Research Network: Kerala, 2006; p 108.
35. Ferro, D. R.; Provasoli, A.; Ragazzi, M.; Casu, B.; Torri, G.; Bossennec, V.; Perly, B.; Sinay, P.; Petitou, M.; Choay, J. *Carbohydr. Res.* **1990**, *195*, 157–167.
36. Engelsen, S. B.; Monteiro, C.; de Penhoat, C. H.; Pérez, S. *Biophys. Chem.* **2001**, *93*, 103–127.
37. Ernst, S.; Venkataraman, G.; Sasisekharan, V.; Langer, R.; Cooney, C. L.; Sasisekharan, R. *J. Am. Chem. Soc.* **1997**, *120*, 2099–2107.
38. Angulo, J.; Nieto, P. M.; Martín-Lomas, M. *Chem. Commun.* **2003**, *13*, 1512–1513.
39. Hricovíni, M.; Scholtzová, E.; Bízik, F. *Carbohydr. Res.* **2007**, *342*, 1350–1356.